J Oceanogr (2016) 72:343–358
DOI 10.1007/s10872-015-0346-9

SPECIAL SECTION: ORIGINAL ARTICLE

K2S1 project

Seasonal variability of phytoplankton community structure in the subtropical western North Pacific

Tetsuichi Fujiki[1] · Kosei Sasaoka[1] · Kazuhiko Matsumoto[2] · Masahide Wakita[3] · Yoshihisa Mino[4]

Received: 23 March 2015 / Revised: 18 December 2015 / Accepted: 24 December 2015 / Published online: 12 January 2016
© The Oceanographic Society of Japan and Springer Japan 2016

Abstract During 2010–2012 in the northwestern region of the North Pacific subtropical gyre, we examined seasonal variability of the phytoplankton community with respect to structure and photo-physiological status using the chemotaxonomy program CHEMTAX and fast-repetition-rate fluorometry. Total chlorophyll *a* standing stock in the upper 150 m (∫TChl *a*) varied from 25.5 to 89.0 mg m^{-2} during periods of relatively deep vertical mixing (40–207 m), but was fairly constant (18.6–27.2 mg m^{-2}) during stratification periods. Prymnesiophytes, chlorophytes, chrysophytes, prasinophytes, and/or diatoms comprised major portions of the ∫TChl *a* during mixing periods. Diatoms became the most abundant group (29–43 %) in February 2011, when large phytoplankton blooms were observed, whereas *Prochlorococcus* was the dominant component (15–46 %) during stratification periods. During mixing periods, nitrate and nitrite (NO_3 + NO_2) concentrations occasionally exceeded 0.5 μmol kg^{-1} in surface waters, and F_v/F_m (photochemical efficiency of photosystem II) ranged from approximately 0.40–0.50 within the euphotic zone. During stratification periods, however, NO_3 + NO_2 concentrations were very low (<0.1 μmol kg^{-1}) from the surface to 50–95 m, and F_v/F_m was in the range of 0.25–0.40 in the upper mixed layer. The seasonal variability of phytoplankton community structure in this region was related to the nutrient supply from deep waters. Additionally, we compared our data to published values at the time-series station ALOHA, located in the eastern region of the NPSG. At Sta. ALOHA in 2011, ∫TChl *a* was almost constant (19.5–26.4 mg m^{-2}) throughout the year and was consistently dominated by *Prochlorococcus* (61–81 %). These results suggest that the phytoplankton community in the northwestern region of the NPSG is seasonally variable and composed of diverse groups compared with the eastern region of the NPSG.

Keywords CHEMTAX · Fast-repetition-rate fluorometry · North Pacific subtropical gyre · Phytoplankton blooms · Pigments

1 Introduction

The North Pacific subtropical gyre (NPSG) is generally considered to be an oligotrophic environment throughout the year because strong stratification of the water column constrains the supply of nutrients from deep water (Eppley et al. 1973; Karl 1999). To investigate the spatial and temporal variability of physical and biogeochemical processes in the NPSG, representative time-series observations (Hawaii Ocean Time-series program) have been carried out at about monthly intervals since October 1988 at Station (Sta.) ALOHA (22°45′N, 158°W; Fig. 1), which is located in the eastern part of the NPSG (Karl and Winn 1991). The time-series observations demonstrated that the eastern part of the NPSG is characterized by a deep

✉ Tetsuichi Fujiki
tfujiki@jamstec.go.jp

1 Research and Development Center for Global Change, Japan Agency for Marine-Earth Science and Technology, 2-15 Natsushima-cho, Yokosuka 237-0061, Japan

2 Department of Environmental Geochemical Cycle Research, Japan Agency for Marine-Earth Science and Technology, 2-15 Natsushima-cho, Yokosuka 237-0061, Japan

3 Mutsu Institute for Oceanography, Japan Agency for Marine-Earth Science and Technology, 690 Kitasekine, Sekine, Mutsu 035-0022, Japan

4 Institute for Space-Earth Environmental Research, Nagoya University, Chikusa-ku, Nagoya 464-8601, Japan

permanent pycnocline, and near-zero concentrations of nitrate and phosphate were routinely observed in the upper 100 m, even in winter when the mixed layer depth was deeper, with the water column being chronically nutrient-starved in the upper mixed layer (Karl and Lukas 1996). In the eastern part of the NPSG, the biomass of the phytoplankton community is low at the surface because of nutrient depletion and forms a deep chlorophyll (Chl) maximum near the top of the nitracline, where nutrient concentrations are sufficient to support growth (Letelier et al. 1993; Corno et al. 2008). Campbell and Vaulot (1993) showed that the phytoplankton community at Sta. ALOHA was numerically dominated by two genera of prokaryotic cells of <2 μm in size, *Prochlorococcus* and *Synechococcus*, which have high surface-area-to-volume ratios that allow them to take up nutrients efficiently. Based on class-specific pigment analysis and electron microscopy, Andersen et al. (1996) found that *Prochlorococcus*-like microorganisms constituted approximately 50 % of concentrations of monovinyl (MV) Chl *a* and divinyl (DV) Chl *a* (hereafter referred as total Chl *a*), and another prokaryote, *Synechococcus*, and two picoeukaryotes, prymnesiophytes and pelagophytes, accounted for most of the rest of total Chl *a*.

Although a long-term time-series station such as Sta. ALOHA has not been established in the western part of the NPSG, several intensive observations characterized this region as having typical oligotrophic conditions, that is, strong stratification, low nutrient concentrations, and low plankton biomass. For instance, Furuya (1990) observed low concentrations (<0.1 mg m^{-3}) of surface Chl *a* and the formation of a deep Chl maximum (>0.2 mg m^{-3}) between 65 and 150 m in the tropical and subtropical western Pacific from August to November 1979. Suzuki et al. (1995) reported that *Prochlorococcus* accounted for >50 % of total Chl *a* within the euphotic zone and generally occurred under conditions of 15–30 °C and 0–10 μM nitrate plus nitrite ($NO_3 + NO_2$) in most of the tropical and subtropical regions along 175°E in August and September 1993. Fujiki et al. (2013) conducted meridional observations along 155°E (between 0 and 24°N) in February and March 2007 and found that the phytoplankton community was dominated by relatively small cells, including *Prochlorococcus*, *Synechococcus*, and picoeukaryotes. Hashihama et al. (2014) used an underway survey system with a highly sensitive nutrient analyzer and showed that the surface concentrations of $NO_3 + NO_2$ and phosphate were typically depleted to <20 μmol L^{-1} in the area along the 155°E transect (between 10 and 35°N) in September 2008.

In contrast, throughout the northwestern region of the NPSG, which is affected by the East Asian winter monsoon, vertical mixing of the water column is enhanced in winter by the increase of heat exchange between the atmosphere and the ocean (e.g., Oka and Qiu 2012). A time series of Chl *a* maps from 1997 to 2013 based on satellite remote sensing of ocean color revealed the occurrence of early spring blooms every year in the northwestern region of the NPSG (Siswanto et al. 2015). However, the seasonal variability in phytoplankton community structure in this region is not well understood, because a series of observations has not been carried out.

In this study, we investigated the seasonal variability of the phytoplankton community (abundance, size, taxonomic composition, and photo-physiological state) in the northwestern region of the NPSG. In addition, we compared our findings with the published data set for Sta. ALOHA and assessed the similarities and differences between the phytoplankton community structure in the northwestern and eastern regions of the NPSG. Our study will provide a better understanding of the mechanisms that regulate seasonal phytoplankton dynamics in the NPSG.

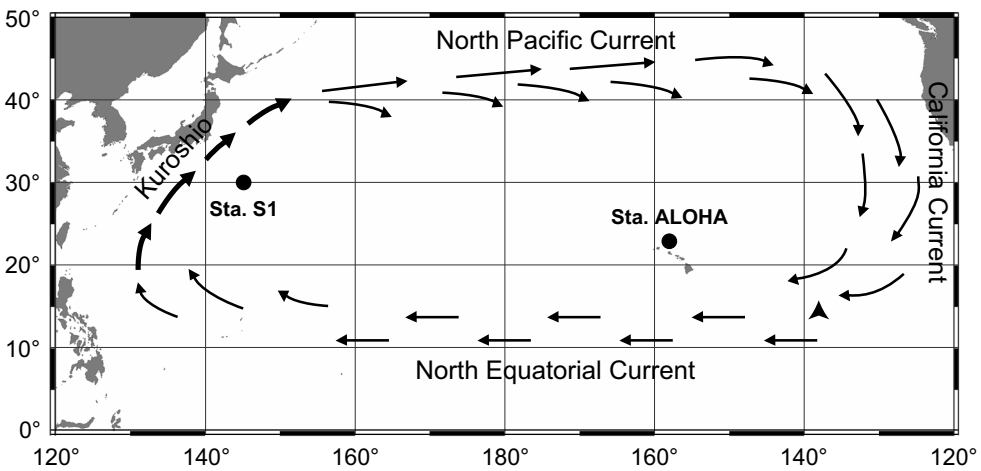

Fig. 1 Locations of time-series Sta. S1 (30°N, 145°E) and Sta. ALOHA (22°45′N, 158°W), and major surface currents in the North Pacific (adapted from Karl 1999)

2 Methods

2.1 Station and water sampling

The observations for this study were conducted during six cruises of the R/V *Mirai* (Japan Agency for Marine-Earth Science and Technology) in the western North Pacific: MR10-01 (20 January–24 February 2010), MR10-06 (18 October–16 November 2010), MR11-02 (11 February–9 March 2011), MR11-03 (14 April–5 May 2011), MR11-05 (27 June–4 August 2011), and MR12-02 (4 June–12 July 2012). Sampling in the upper 200 m was performed at time-series Sta. S1 (30°N, 145°E; Fig. 1) in the northwestern region of the NPSG before dawn using a bucket (surface only) and 12-L Niskin-X bottles (General Oceanics, Miami, FL, USA) attached to a conductivity–temperature–depth sensor (911 plus, Sea-Bird Electronics, Bellevue, WA, USA) carousel system. The seawater samples were analyzed onboard with a continuous flow analyzer (QuAAtro 2-HR, BL TEC, Tokyo, Japan). Concentrations of $NO_3 + NO_2$ were quantified using the reference materials for nutrients in seawater (General Environmental Technos, Osaka, Japan). The detection limit for $NO_3 + NO_2$, estimated as being three times the standard deviation of blank water, was 0.06 μmol kg^{-1}. Seawater collected from the surface of the NPSG and preserved for >1 year was used as the $NO_3 + NO_2$ blank. The precision for $NO_3 + NO_2$ at 0.1 and 6.2 μmol kg^{-1} (the reference materials) had coefficients of variation of 23 and 0.8 %, respectively.

We used continuous vertical profiles of potential density to calculate the mixed layer depth (MLD), which we equated to the depth at which the density was 0.125 kg m^{-3} greater than the density at the surface (de Boyer et al. 2004). The depth of the top of the nitracline was defined as the shallowest depth at which the $NO_3 + NO_2$ concentration exceeded 0.1 μmol kg^{-1} (Campbell and Vaulot 1993). In addition, the euphotic layer depth (ELD) was defined as the depth where the irradiance was diminished to 1 % of the surface value (Ryther 1956), and it was determined by using a sea-viewing wide field-of-view sensor (SeaWiFS) profiling multichannel radiometer (SPMR), and multichannel surface reference sensor (SMSR) (Satlantic, Halifax, Nova Scotia, Canada) during daylight on the day before the seawater sampling.

The microwave optically interpolated (MWOI) sea-surface temperature (SST) products and Chl *a* concentrations of the moderate resolution imaging spectroradiometer (MODIS) between January 2003 and December 2012 in an area of about 10,000 km^2 centered at Sta. S1 and Sta. ALOHA were obtained from Remote Sensing Systems (http://www.remss.com/) and NASA's Ocean Color Web (http://oceancolor.gsfc.nasa.gov/), respectively. We used the Interactive Data Language program (Exelis Visual Information Solutions, Boulder, CO, USA) to calculate the mean SST and Chl *a* values of each 11 × 11 pixels square box (about 100 × 100 km).

2.2 Variable fluorescence measurements

Single-turnover fluorescence induction curves of photosystem (PS) II were measured using a fast-repetition-rate fluorometer (Diving Flash, Kimoto Electric, Osaka, Japan). Details about the instrument and measurement protocol were described by Fujiki et al. (2008). Before dawn, we obtained vertical profiles of fluorescence induction curves at intervals of approximately 1 m by lowering the instrument through the water column to a depth of 120 m and then raising the instrument at a rate of 0.2 m s^{-1} with the ship's winch. In this study, we used the data from the upward casts. Potential photochemical efficiency of PSII (F_v/F_m) was calculated from the fluorescence induction curve by using the numerical fitting procedure described by Kolber et al. (1998). A high value of F_v/F_m means that energy losses (as heat and fluorescence) are low and that absorbed light energy is being efficiently used in photosynthesis.

2.3 Pigment analysis

Samples for algal pigment analyses were collected from 8 to 14 depths within the upper 150 m. For high-performance liquid chromatography (HPLC) measurements, seawater samples of 2–5 L were filtered through glass fiber filters (GF/F, Whatman International, Kent, UK) under gentle vacuum (<0.02 MPa). The filters were dehydrated by freeze-drying at 0 °C and then extracted with 4 mL *N,N*-dimethylformamide (DMF) for at least 24 h at −20 °C in the dark. We used DMF as a solvent because its strong extractability promotes the extraction process and thus prevents the loss of pigments (Furuya et al. 1998). The extracts were filtered through 0.2-μm pore size hydrophile polytetrafluoroethylene membrane filters (Millex-LG, Millipore Corp., Billerica, MA, USA) to remove cellular debris and glass fibers. The filtrate was mixed with distilled-deionized water in a 7:3 volume ratio to achieve sufficient retention and optimal resolution for HPLC pigment analysis. The mixtures were analyzed on board with an HPLC modular system (Waters, Milford, MA, USA, during cruise MR10-01 and Agilent, Santa Clara, CA, USA, during the other cruises) that included a C8 column containing pyridine in the mobile phase (Zapata et al. 2000). Pigment concentrations were quantified using commercially available standards (Danish Hydraulic Institute Water and Environment, Hørsholm, Denmark). Because the HPLC method employed was not capable of separating MVChl *b* and DVChl *b*, we estimated

Table 1 Initial and final biomarker pigment-to-Chl *a* ratios for eight algal groups at Sta. S1 based on CHEMTAX analysis

	Peri	Fucox	19′-But	19′-Hex	Diadi	Prasi	Zeax	Chl *b*	DVChl *a*	Chl *a*
Initial										
Dinoflagellates	1.10	–	–	–	0.24	–	–	–	–	1.00
Diatoms	–	0.75	–	–	0.14	–	–	–	–	1.00
Chrysophytes	–	0.35	0.76	–	0.19	–	–	–	–	1.00
Prymnesiophytes	–	–	–	1.70	0.10	–	–	–	–	1.00
Prasinophytes	–	–	–	–	–	0.32	–	0.95	–	1.00
Chlorophytes	–	–	–	–	–	–	0.01	0.26	–	1.00
Cyanobacteria	–	–	–	–	–	–	0.35	–	–	1.00
Prochlorococcus	–	–	–	–	–	–	0.32	1.10	1.00	–
Final										
Mixing period										
Dinoflagellates	1.10	–	–	–	0.24	–	–	–	–	1.00
Diatoms	–	0.75	–	–	0.06	–	–	–	–	1.00
Chrysophytes	–	0.35	1.04	–	0.07	–	–	–	–	1.00
Prymnesiophytes	–	–	–	1.70	0.11	–	–	–	–	1.00
Prasinophytes	–	–	–	–	–	0.32	–	0.80	–	1.00
Chlorophytes	–	–	–	–	–	–	0.01	0.17	–	1.00
Cyanobacteria	–	–	–	–	–	–	0.62	–	–	1.00
Prochlorococcus	–	–	–	–	–	–	0.32	0.64	1.00	–
Stratification period										
Dinoflagellates	1.10	–	–	–	0.24	–	–	–	–	1.00
Diatoms	–	0.55	–	–	0.44	–	–	–	–	1.00
Chrysophytes	–	0.30	1.35	–	0.04	–	–	–	–	1.00
Prymnesiophytes	–	–	–	1.16	0.05	–	–	–	–	1.00
Prasinophytes	–	–	–	–	–	0.75	–	0.61	–	1.00
Chlorophytes	–	–	–	–	–	–	0.04	1.49	–	1.00
Cyanobacteria	–	–	–	–	–	–	1.08	–	–	1.00
Prochlorococcus	–	–	–	–	–	–	0.23	0.20	1.00	–

The calculation was made separately for each phytoplankton community during the mixing and stratification periods

Peri peridinin, *Fucox* fucoxanthin, *19′-But* 19′-butanoyloxyfucoxanthin, *19′-Hex* 19′-hexanoyloxyfucoxanthin, *Diadi* diadinoxanthin, *Prasi* prasinoxanthin, *Zeax* zeaxanthin, *Chl b* chlorophyll *b*, *DVChl a* divinyl chlorophyll *a*, *Chl a* chlorophyll *a*

the concentrations of total Chl *b* (hereafter referred to as "Chl *b*") with the response factor determined for MVChl *b*.

For size-fractionated Chl *a* determination, we filtered 1-L seawater samples sequentially through Nuclepore filters (Whatman International) with pore sizes of 10 and 3 μm and then through a Whatman GF/F filter (nominal pore size of 0.7 μm) under gentle vacuum (<0.02 MPa). Each filter was extracted in DMF (Suzuki and Ishimaru 1990), and Chl *a* concentrations were measured with a fluorometer (model 10-AU, Turner Designs, Sunnyvale, CA, USA) using the methodology described by Welschmeyer (1994). The relative Chl *a* contribution from each size fraction was expressed as a percentage of the sum of the Chl *a* in all three fractions. The Chl *a* reported here is the sum of DVChl *a* and MVChl *a*. In this method, the latter was not separately determined.

2.4 Determination of phytoplankton groups by CHEMTAX

By using the chemotaxonomy program CHEMTAX (Mackey et al. 1996), the contribution of each phytoplankton group to the concentration of total Chl *a* was estimated from the concentrations of biomarker pigments measured with the HPLC. Eight algal groups were separated based on their pigment ratios (Table 1). Initial pigment ratios were derived from Miki et al. (2008), who previously used CHEMTAX for analysis of pigments in oligotrophic waters of the western North Pacific. Because DVChl *a* is a unique biomarker pigment for *Prochlorococcus*, this genus was distinguished from other cyanobacteria in the CHEMTAX analysis, and; hence, the cyanobacteria in this study do not include

Table 2 Initial and final biomarker pigment-to-Chl *a* ratios for eight algal groups at Sta. ALOHA based on CHEMTAX analysis

	Peri	Fucox	19′-But	19′-Hex	Diadi	Prasi	Zeax	Chl *b*	DVChl *a*	Chl *a*
Initial										
Dinoflagellates	1.10	–	–	–	0.24	–	–	–	–	1.00
Diatoms	–	0.75	–	–	0.14	–	–	–	–	1.00
Chrysophytes	–	0.35	0.76	–	0.19	–	–	–	–	1.00
Prymnesiophytes	–	–	–	1.70	0.10	–	–	–	–	1.00
Prasinophytes	–	–	–	–	–	0.32	–	0.95	–	1.00
Chlorophytes	–	–	–	–	–	–	0.01	0.26	–	1.00
Cyanobacteria	–	–	–	–	–	–	0.35	–	–	1.00
Prochlorococcus	–	–	–	–	–	–	0.32	1.10	1.00	–
Final										
Dinoflagellates	1.10	–	–	–	0.24	–	–	–	–	1.00
Diatoms	–	0.66	–	–	0.35	–	–	–	–	1.00
Chrysophytes	–	0.18	1.77	–	0.19	–	–	–	–	1.00
Prymnesiophytes	–	–	–	1.70	0.10	–	–	–	–	1.00
Prasinophytes	–	–	–	–	–	0.32	–	0.95	–	1.00
Chlorophytes	–	–	–	–	–	–	0.01	0.26	–	1.00
Cyanobacteria	–	–	–	–	–	–	0.35	–	–	1.00
Prochlorococcus	–	–	–	–	–	–	0.41	0.60	1.00	–

See Table 1 for abbreviation definitions

Prochlorococcus. Following the procedures described by Latasa (2007) and Latasa et al. (2010), the output of each run was used as input for the following run, and this procedure was repeated five times. In this study, the calculation was made separately for each phytoplankton community at Sta. S1 during the mixing and stratification periods. The pigment ratios of each algal group were assumed to be independent of depth. Finally, we calculated the relative contribution of each algal group to the integral of total Chl *a* within the upper 150 m.

2.5 Microscopic examination

During cruise MR11-02, when large spring blooms were observed, 500 mL of seawater was fixed with neutralized formalin (final concentration, 1 %). These samples were concentrated to 10 mL by settling, and phytoplankton were counted and identified under an inverted light microscope. Because of the formalin fixative and magnification of the light microscope (approximately 400×), the identification of phytoplankton was limited to diatoms larger than 10 μm.

2.6 Sta. ALOHA data set

To examine the similarities and differences between phytoplankton community structure in the northwestern and eastern regions of the NPSG, we obtained the data sets of phytoplankton pigments and environmental factors (temperature, salinity, and $NO_3 + NO_2$) at Sta. ALOHA (Fig. 1) in 2011 from the Hawaii Ocean Time-series Data Organization and Graphical System (http://hahana.soest.hawaii.edu/hot/hot-dogs/interface.html). By using the CHEMTAX program, we calculated the contribution of each algal group to total Chl *a* at Sta. ALOHA in the same manner as for Sta. S1. Note, however, that the pigment ratios of each algal group at Sta. ALOHA were assumed to be constant throughout the year because the upper water column was stratified throughout the year (Table 2).

3 Results and discussion

3.1 Satellite data and water mass characteristics

On the basis of the MWOI SST product data from 2003 to 2012, the SST in an area of about 100 km^2 centered on Sta. S1 was almost constant and was in the range of 18–21 °C between January and May (Fig. 2a). The SST increased to about 28 °C by August and then decreased gradually after October. A time series of Chl *a* maps from MODIS during the same period showed a different pattern. Surface Chl *a* around Sta. S1 was relatively high and ranged from 0.1 to 0.4 mg m^{-3} between January and May (>0.5 mg m^{-3} early in April 2004 and 2011) and decreased to about 0.05 mg m^{-3} between July and November (Fig. 2c). In contrast, the SST around Sta. ALOHA ranged from approximately 23–27 °C (Fig. 2b); the seasonal variation in SST was relatively small compared to that of Sta. S1. Except for the transient Chl *a* peaks in the summer of 2005 and 2006,

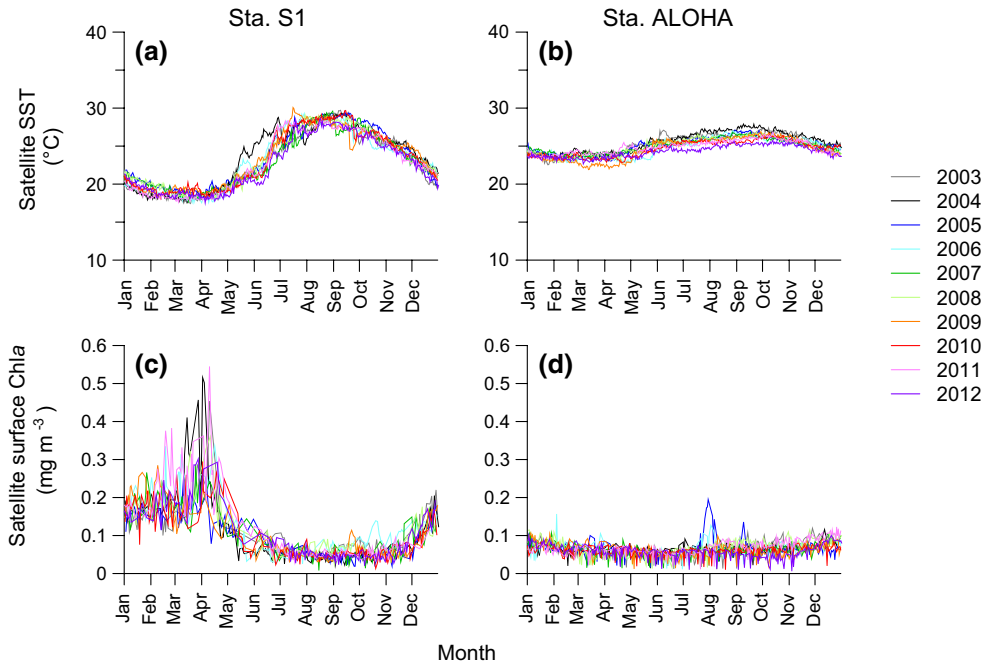

Fig. 2 Seasonal variations of **a**, **b** sea-surface temperatures (SSTs) and **c**, **d** Chl *a* concentrations between 2003 and 2012 in areas of about 10,000 km^2 centered at Sta. S1 and Sta. ALOHA based on satellite image data from the MWOI SST product and MODIS, respectively

surface Chl *a* concentrations around Sta. ALOHA were relatively constant and remained at low levels (<0.1 mg m^{-3}) throughout the year (Fig. 2d).

Vertical profiles of environmental characteristics at Sta. S1 were determined from shipboard observations. Temperature ranged from 17 to 20 °C in the upper 200 m between February and May and decreased slightly with depth (Fig. 3a), but a relatively strong thermocline was formed in the upper 60 m between June and November (Fig. 3b). Salinity ranged from 34.65 to 34.80 in the upper 200 m between February and May (Fig. 3c); low salinity (<34.65) was recorded in the upper 60 m between June and November (Fig. 3d). The MLD ranged from 71 to 207 m between February and April and was relatively shallow (13–21 m) between June and July (Table 3). In February, $NO_3 + NO_2$ concentrations usually exceeded 0.5 μmol kg^{-1} in the surface waters due to influxes of nutrient-rich deep waters (Fig. 3e). In contrast, between June and November, $NO_3 + NO_2$ concentrations were low (<0.1 μmol kg^{-1}) from just below the surface to 50–95 m and increased rapidly in the lower region of the euphotic zone (Fig. 3f). Because we observed seasonal variability in water mass structure, we divided the data collected during this study into two periods: the mixing period (February–May) and the stratification period (June–November). The ELD ranged from 70 to 86 m during the mixing period and then deepened to between 91 and 111 m during the stratification period (Table 3).

At Sta. ALOHA, temperature in the upper 50 m was roughly constant throughout the year, and the values ranged from 24 to 26 °C (Fig. 4a). Salinity was >35.00 in the upper 100 m, except in July, and was relatively higher than that at Sta. S1 (Fig. 4b). Despite the MLD deepening to below 100 m between November and December (Table 4), $NO_3 + NO_2$ concentrations in the upper 100 m remained low (usually <0.1 μmol kg^{-1}) throughout the year (Fig. 4c).

3.2 Phytoplankton physiological state at Sta. S1

The potential photochemical efficiency of PSII, F_v/F_m, has been generally used as an indicator of nutrient stress (e.g., Cleveland and Perry 1987; Geider et al. 1993). At Sta. S1, during the mixing period, when nutrients were supplied from deeper waters to the surface layer, F_v/F_m above the ELD was relatively high and ranged between 0.40 and 0.50, except on 1 May 2011 (Fig. 5a). However, during the stratification period, when the nutrient supply from deep waters was restricted, F_v/F_m was <0.40 in the mixed layer and ranged between 0.25 and 0.35 at shallower depths, except on 8 November 2010 (Fig. 5b). These features of the F_v/F_m profiles indicate that nutrients were less limiting to phytoplankton growth during the mixing period but became more limiting in the upper mixed layer during the stratification period.

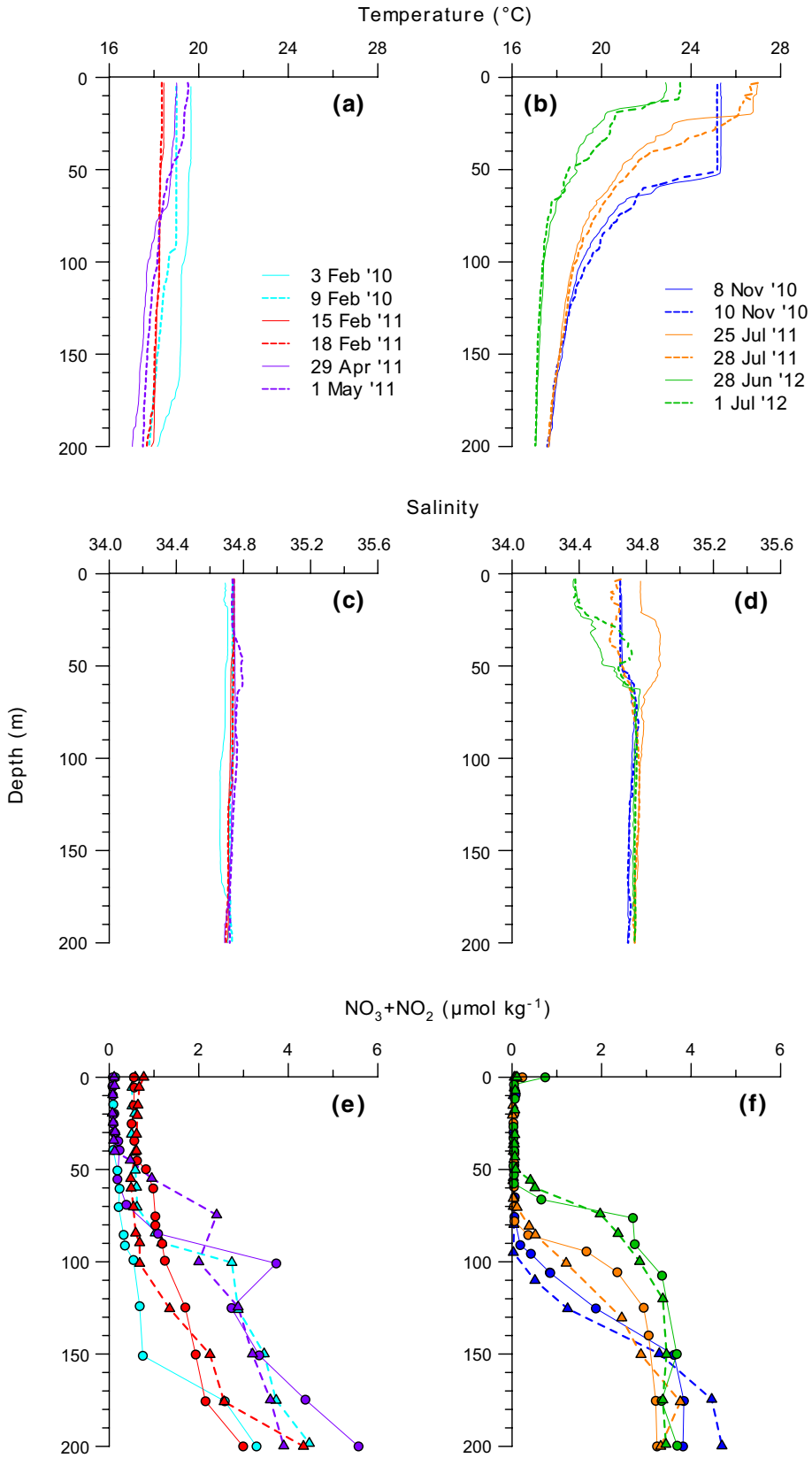

Fig. 3 Vertical profiles of **a**, **b** temperature, **c**, **d** salinity, and **e**, **f** nitrate + nitrite concentration at Sta. S1 during the mixing period (February–May) and the stratification period (June–November)

Table 3 Summary of the mixed layer depth (MLD), euphotic layer depth (ELD), nitracline depth, ∫TChl *a*, and the size and taxonomic group composition of phytoplankton at Sta. S1 during the mixing and stratification periods

Period	Date		MLD (m)	ELD (m)	Nitracline (m)	∫TChl *a* (mg m^{-2})	Size composition (%)			Group composition (%)							
							>10 µm	3–10 µm	<3 µm	Dino	Diato	Chryso	Prymne	Prasino	Chloro	Cyano	Prochloro
Mixing	2010	3 Feb	164	71	20	41.1	7.3	14.0	78.7	1.3	2.0	13.7	17.7	16.1	17.5	15.7	16.1
		9 Feb	112	71	0	36.6	9.4	12.4	78.2	1.9	4.3	11.9	20.8	17.7	18.2	11.1	14.2
	2011	15 Feb	207	61	0	56.5	42.9	12.4	44.7	1.8	28.6	13.1	13.7	13.7	22.0	4.5	2.7
		18 Feb	196	70	0	89.0	54.8	11.2	34.0	2.1	42.8	11.3	13.1	7.5	18.1	3.5	1.6
		29 Apr	71	56	30	51.4	13.3	13.4	73.4	1.9	6.9	17.0	28.3	15.9	17.9	8.3	3.8
		1 May	40	55	30	25.5	15.6	12.5	71.9	2.1	4.9	22.3	25.7	10.5	12.8	16.2	5.5
Stratification	2010	8 Nov	54	90	96	18.6	–	–	–	2.1	2.1	11.2	14.6	0.8	17.4	6.8	45.1
		10 Nov	52	95	110	19.4	4.1	6.7	89.2	2.6	1.8	10.6	15.3	0.9	16.4	6.6	46.0
	2011	25 Jul	21	95	86	22.4	12.2	10.6	77.2	1.8	2.3	16.1	18.8	2.0	22.5	8.6	27.8
		28 Jul	17	86	71	27.2	11.7	10.9	77.5	1.5	2.2	16.6	19.4	2.0	20.1	9.8	28.4
	2012	28 Jun	14	77	66	23.2	5.8	13.5	80.6	1.7	2.6	16.3	20.5	1.6	17.6	11.8	27.8
		1 Jul	13	85	56	19.6	6.5	16.3	77.3	2.6	2.6	21.7	29.5	2.6	13.6	12.0	15.4

The ∫TChl *a*, size composition, and group composition are depth-integrated values within the upper 150 m. On 3 and 9 February and 8 November 2010 and 29 April, 1 May, and 25 July 2011, when the deepest depth of sampling was shallower than 150 m, the Chl *a* concentration at 150 m was assumed to be zero

Dino dinoflagellates, *Diato* diatoms, *Chryso* chrysophytes, *Prymne* prymnesiophytes, *Prasino* prasinophytes, *Chloro* chlorophytes, *Cyano* cyanobacteria, *Prochloro Prochlorococcus*

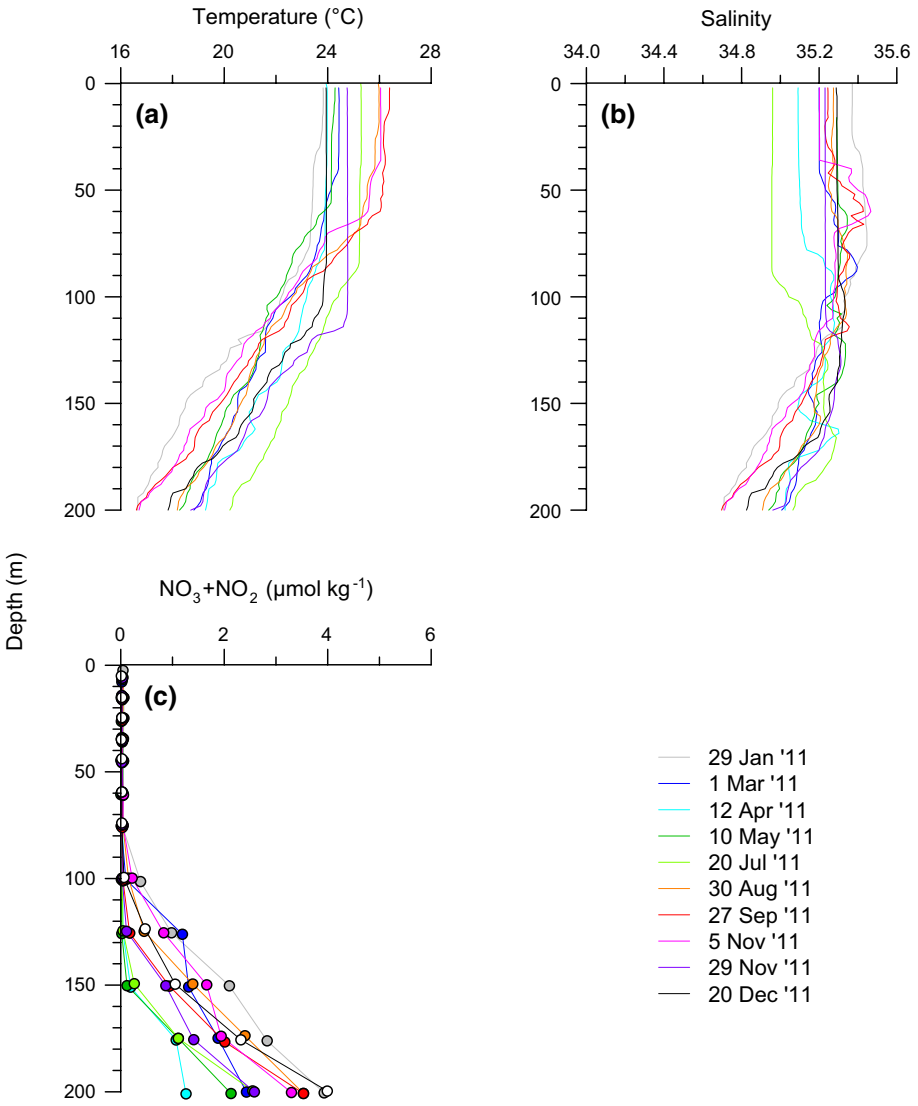

Fig. 4 Vertical profiles of **a**, **b** temperature, **c**, **d** salinity, and **e**, **f** nitrate + nitrite concentration at Sta. ALOHA in 2011

Table 4 Summary of the MLD, ∫TChl *a*, and the taxonomic group composition of phytoplankton at Sta. ALOHA in 2011

Date	MLD (m)	∫TChl *a* (mg m^{-2})	Group composition (%)							
			Dino	Diato	Chryso	Prymne	Prasino	Chloro	Cyano	Prochloro
2011										
29 Jan	36	20.3	1.1	4.1	9.1	16.0	0.6	3.7	4.4	61.0
1 Mar	52	20.3	0.6	3.8	8.6	11.4	0.6	2.3	3.4	69.3
12 Apr	80	19.5	0.4	5.8	4.1	6.4	0.3	0.2	1.5	81.4
10 May	60	23.8	0.6	2.1	8.2	11.2	0.6	3.2	1.5	72.6
20 Jul	92	20.0	0.8	4.7	5.2	10.3	0.3	0.5	5.0	73.2
30 Aug	52	24.6	0.5	1.9	6.7	10.3	0.3	1.9	3.0	75.3
27 Sep	48	24.7	0.6	1.7	5.3	10.8	0.0	0.5	4.9	76.2
5 Nov	40	21.3	0.5	1.2	7.6	10.1	0.7	2.1	1.1	76.8
29 Nov	116	26.4	0.4	1.7	7.9	10.8	0.3	0.8	1.1	77.0
20 Dec	110	20.2	0.5	1.6	6.8	10.4	0.0	1.3	0.5	79.0

See Table 3 for abbreviation definitions

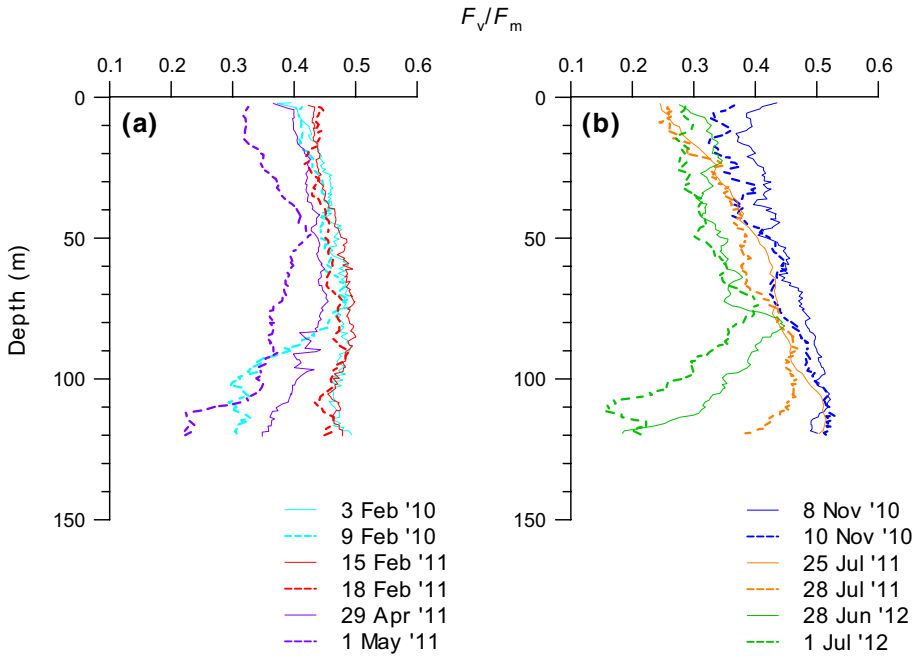

Fig. 5 Vertical profiles of F_v/F_m at Sta. S1 during the **a** mixing period and **b** stratification period

3.3 Phytoplankton pigments and composition

3.3.1 Sta. S1

During this study we measured the concentrations of ten pigments with the HPLC system (Table 1). The highest concentrations (>0.1 mg m^{-3}) were detected for Chl *a*, fucoxanthin (Fucox), 19′-hexanoyloxyfucoxanthin (19′-Hex), 19′-butanoyloxyfucoxanthin (19′-But), Chl *b*, and DVChl *a* (Fig. 6). During the mixing period, Chl *a* concentrations ranged from 0.11 to 0.81 mg m^{-3} and were characterized by almost homogenous concentrations within the euphotic zone, except on 1 May 2011, when a Chl *a* peak was apparent in the vicinity of 45 m (Fig. 6a). High concentrations (>0.6 mg m^{-3}) of Chl *a* were observed in February 2011, coincident with increased Fucox concentrations (Fig. 6c). On 1 May 2011, the Chl *a* peak at about 45 m was accompanied by an increase in concentrations of 19′-Hex, 19′-But, and Chl *b* (Fig. 6e, g, i). The concentrations of DVChl *a* were below 0.1 mg m^{-3} and showed little variation within the upper 150 m (Fig. 6k). In contrast, during the stratification period, Chl *a* concentrations were <0.1 mg m^{-3} in the water column above 40 m but increased sharply to around 0.3 mg m^{-3} between 50 and 90 m in June and July (Fig. 6b). The deep Chl maximum was located near the top of the nitracline, where the effects of nutrient limitation are diminished (Table 3). The concentrations of Fucox were low (<0.04 mg m^{-3}) in the upper 150 m (Fig. 6d), but concentrations of 19′-Hex, 19′-But, and Chl *b* increased markedly at depths below 50 m and occasionally reached as high as >0.1 mg m^{-3} (Fig. 6f, h, j). As was the case with Chl *a*, the vertical profile of DVChl *a* concentrations was characterized by low values (<0.06 mg m^{-3}) from the surface to 40 m and a distinct peak of >0.1 mg m^{-3} at depths near the top of the nitracline (Table 3; Fig. 6l).

The depth-integrated total Chl *a* within the upper 150 m (∫TChl *a*) was in the range of 18.6–89.0 mg m^{-2} during the six cruises (Table 3). Although ∫TChl *a* was quite variable during the mixing period, ∫TChl *a* was relatively high (>36 mg m^{-2}), except for 1 May 2011, indicating that phytoplankton blooms were occurring. In particular, ∫TChl *a* value as high as 89.0 mg m^{-2} was observed in February 2011, when the MLD deepened to about 200 m and the $NO_3 + NO_2$ concentrations exceeded 0.5 μmol kg^{-1} in the surface waters. The >10-μm size fraction of the ∫TChl *a* increased to 43–55 % in February 2011, suggesting that the bloom development was mainly due to an increase of large phytoplankton. In contrast, the ∫TChl *a* was relatively constant (18.6–27.2 mg m^{-2}) during the stratification period. The contribution of the <3-μm size fraction accounted for 77–89 % of the ∫TChl *a*, indicating that picoplankton consistently dominated the phytoplankton composition during the stratification period.

The results of CHEMTAX analysis showed that diatoms were the dominant phytoplankton group, accounting for 29–43 % of ∫TChl *a* in February 2011 during the mixing period, when distinct phytoplankton blooms were observed (Table 3). Microscopic examination of the large diatoms (>10 μm) showed that *Chaetoceros* spp. and *Pseudo-nitzschia* spp. dominated numerically during the phytoplankton blooms (Table 5). Chlorophytes, prymnesiophytes, and chrysophytes accounted for 18–22, 13–14, and

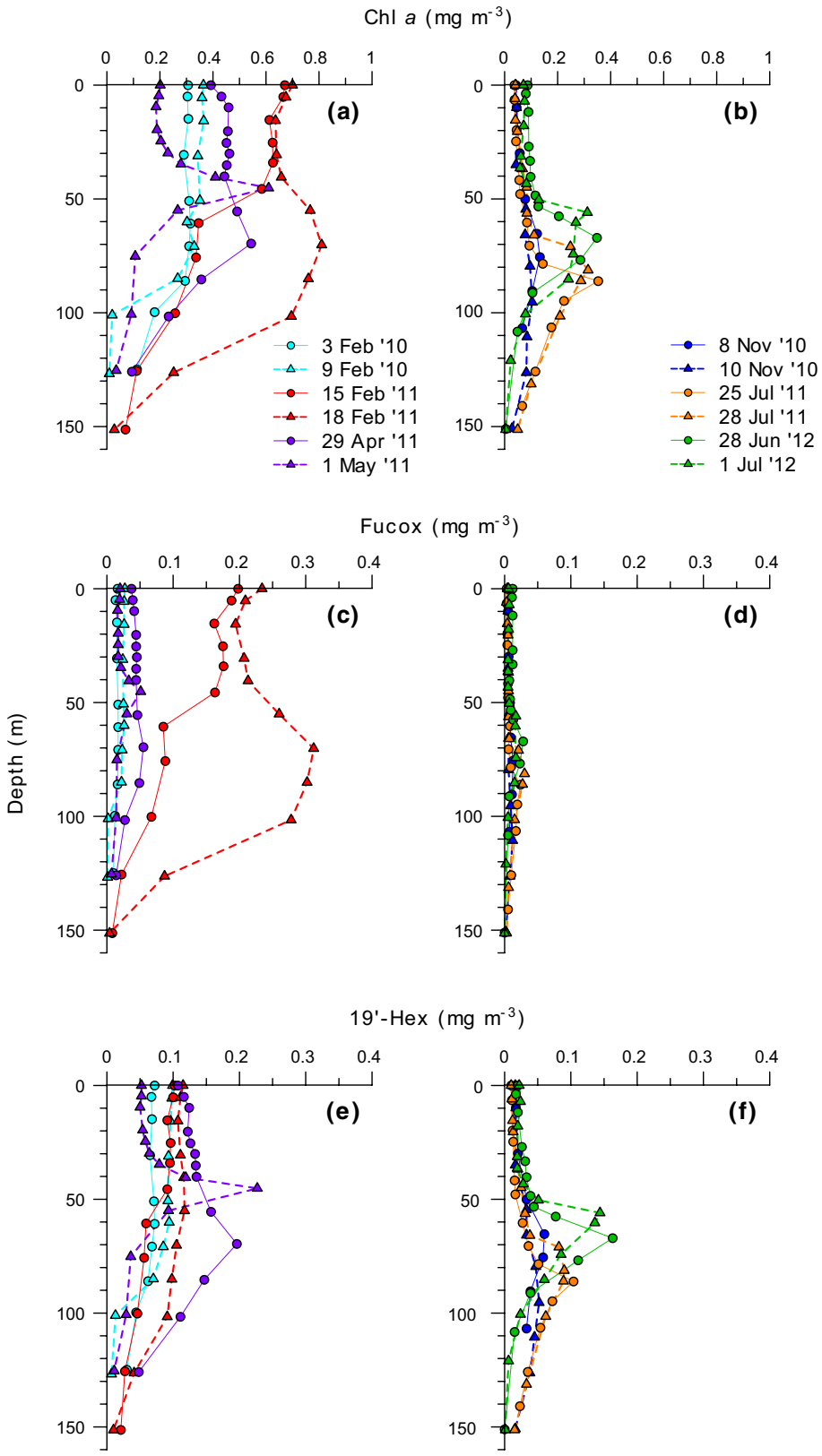

Fig. 6 Vertical profiles of concentrations of **a**, **b** Chl *a*, **c**, **d** Fucox, **e**, **f** 19′-Hex, **g**, **h** 19′-But, **i**, **j** Chl *b*, and **k**, **l** DVChl *a* at Sta. S1 during the mixing period and the stratification period

11–13 % of ∫TChl *a*, respectively, in February 2011 and were groups of secondary importance in the phytoplankton blooms (Table 3). These three groups were distributed in high proportions (chlorophytes: 13–23 %; prymnesiophytes: 15–30 %; chrysophytes: 11–22 %) throughout the year, whereas the contribution of diatoms was very low

Fig. 6 continued

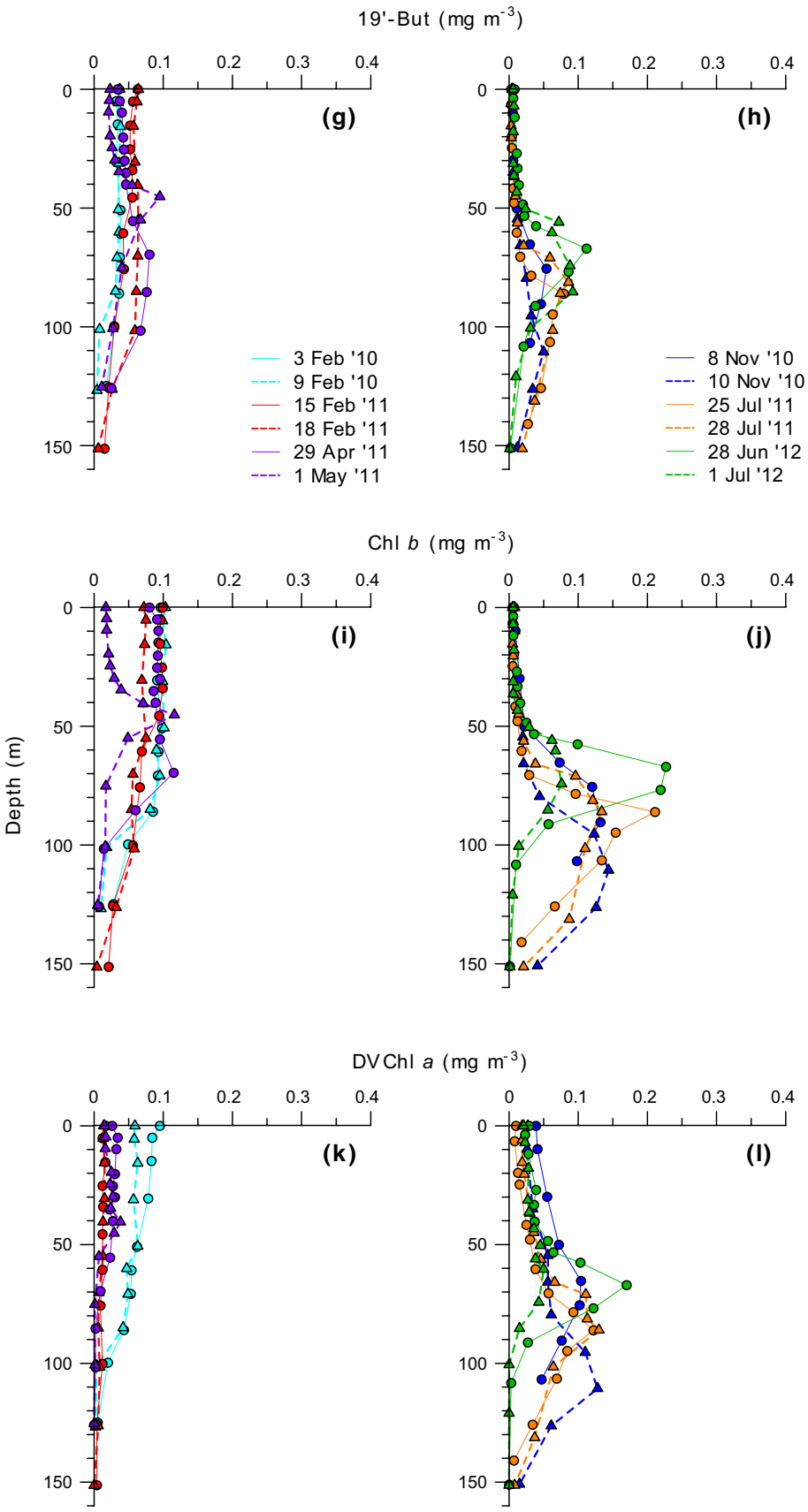

Table 5 Abundance ($\times 10^5$ cells m^{-2}) of the main diatom species within the upper 150 m at Sta. S1 during phytoplankton blooms based on light microscope analysis

Species	2011	
	15 Feb	18 Feb
Centric diatoms		
Bacteriastrum spp.	619	1211
Chaetoceros spp.	1596	2740
Eucampia spp.	267	613
Guinardia spp.	191	228
Thalassiosira spp.	80	763
Pennate diatoms		
Nitzschia spp.	107	378
Pseudo-nitzschia spp.	1472	1838
Thalassionema spp.	396	396

(2–7 %), except for February 2011. The contribution of prasinophytes was in the range of 1–18 % and was higher during the mixing period compared to the stratification period. Dinoflagellates were a minor component throughout the year and accounted for <3 % of the ∫TChl *a*. Cyanobacteria accounted for 4–16 % of the ∫TChl *a*, a contribution that changed very little throughout the year, but the dominance of *Prochlorococcus* changed markedly, from 2–16 % during the mixing period to 15–46 % during the stratification period.

3.3.2 Sta. ALOHA

At Sta. ALOHA, Chl *a* concentrations were <0.05 mg m^{-3} in the water column above 60 m throughout the year, but increased occasionally to >0.1 mg m^{-3} at depths of 100–120 m (Fig. 7a). The concentrations of Fucox, 19′-Hex, 19′-But, and Chl *b* showed little variation (<0.05 mg m^{-3}) within the upper 60 m, but increases in 19′-Hex, 19′-But, and Chl *b* concentrations were observed at depths below 70 m (Fig. 7b–e). The concentrations of DVChl *a* ranged from 0.03 to 0.18 mg m^{-3} even in the surface waters, and distinct peaks with >0.2 mg m^{-3} were observed at depths between 70 and 130 m (Fig. 7f).

The ∫TChl *a* was in the range of 19.5–26.4 mg m^{-2} and was almost constant throughout the year (Table 4). Although the size composition of the phytoplankton community at Sta. ALOHA was not assessed in the present study, Li et al. (2011) found that picoplankton (0.2–2 μm) were dominant contributors throughout the year and accounted for 91 ± 2 % (mean ± SD) of the depth-integrated total Chl *a* within the upper 125 m.

Our CHEMTAX analysis revealed that *Prochlorococcus* accounted for 61–81 % of ∫TChl *a* and was consistently the dominant phytoplankton group at Sta. ALOHA (Table 4). Prymnesiophytes and chrysophytes were secondary components and accounted for a relatively constant proportion (prymnesiophytes: 6–11 %; chrysophytes: 4–9 %) of ∫TChl *a* throughout the year. Dinoflagellates, diatoms, prasinophytes, chlorophytes, and cyanobacteria were minor components throughout the year and accounted for <5 % of the ∫TChl *a*.

3.4 Comparison of Sta. S1 and Sta. ALOHA

Our study revealed both similarities and differences in the phytoplankton community structure at Sta. S1 and Sta. ALOHA. First, the ∫TChl *a* at Sta. S1 was nearly constant (18.6–27.2 mg m^{-2}) during the stratification period (Table 3) and was similar to that (19.5–26.4 mg m^{-3}) at Sta. ALOHA, which showed little change throughout the year (Table 4). Second, *Prochlorococcus* was the dominant phytoplankton group in terms of total Chl *a* standing stock during the stratification period at Sta. S1 (Table 3) and throughout the year at Sta. ALOHA (Table 4). The contribution of *Prochlorococcus* was as high as 81 % at Sta. ALOHA, but was in the range of 15–46 % at Sta. S1. The proportions of prymnesiophytes, chlorophytes, and chrysophytes at Sta. S1 were relatively high compared to those at Sta. ALOHA, indicating that the phytoplankton community at Sta. S1 comprised diverse groups even during the stratification period, when ∫TChl *a* was relatively low. Finally, a notable difference between the two stations was the occurrence of seasonal phytoplankton blooms. Although the lack of seasonal variation in ∫TChl *a* was confirmed at Sta. ALOHA (Table 4), high ∫TChl *a* values (25.5–89.0 mg m^{-2}) have been observed during the mixing period at Sta. S1 (Table 3). At Sta. S1, the top of the nitracline was in the range of 56–110 m during the stratification period, but shoaled drastically to about 0–30 m during the mixing period. In addition, we found that F_v/F_m at shallower depths was relatively high (>0.4) during the mixing period compared to the stratification period (Fig. 5), suggesting that the stress from nutrient limitation was reduced by a nutrient supply from deeper waters. At Sta. ALOHA, although the top of the nitracline was not determined because of wide sampling-depth intervals (approximately 25 m) below 75-m depth, $NO_3 + NO_2$ concentrations were <0.1 μmol kg^{-1} within the upper 75 m throughout the year. Corno et al. (2008) conducted fast-repetition-rate fluorometric measurements at Sta. ALOHA quasi-monthly (between 3 and 5 weeks) from September 2002 to December 2004. They found that F_v/F_m showed no distinct seasonal variation and was as low as 0.37 ± 0.01 in the surface layer (0–10 m), resulting in chronic nutrient limitation of phytoplankton growth. The presence/absence of seasonal blooms at Sta. S1 and Sta. ALOHA was therefore probably due to the difference in nutrient conditions.

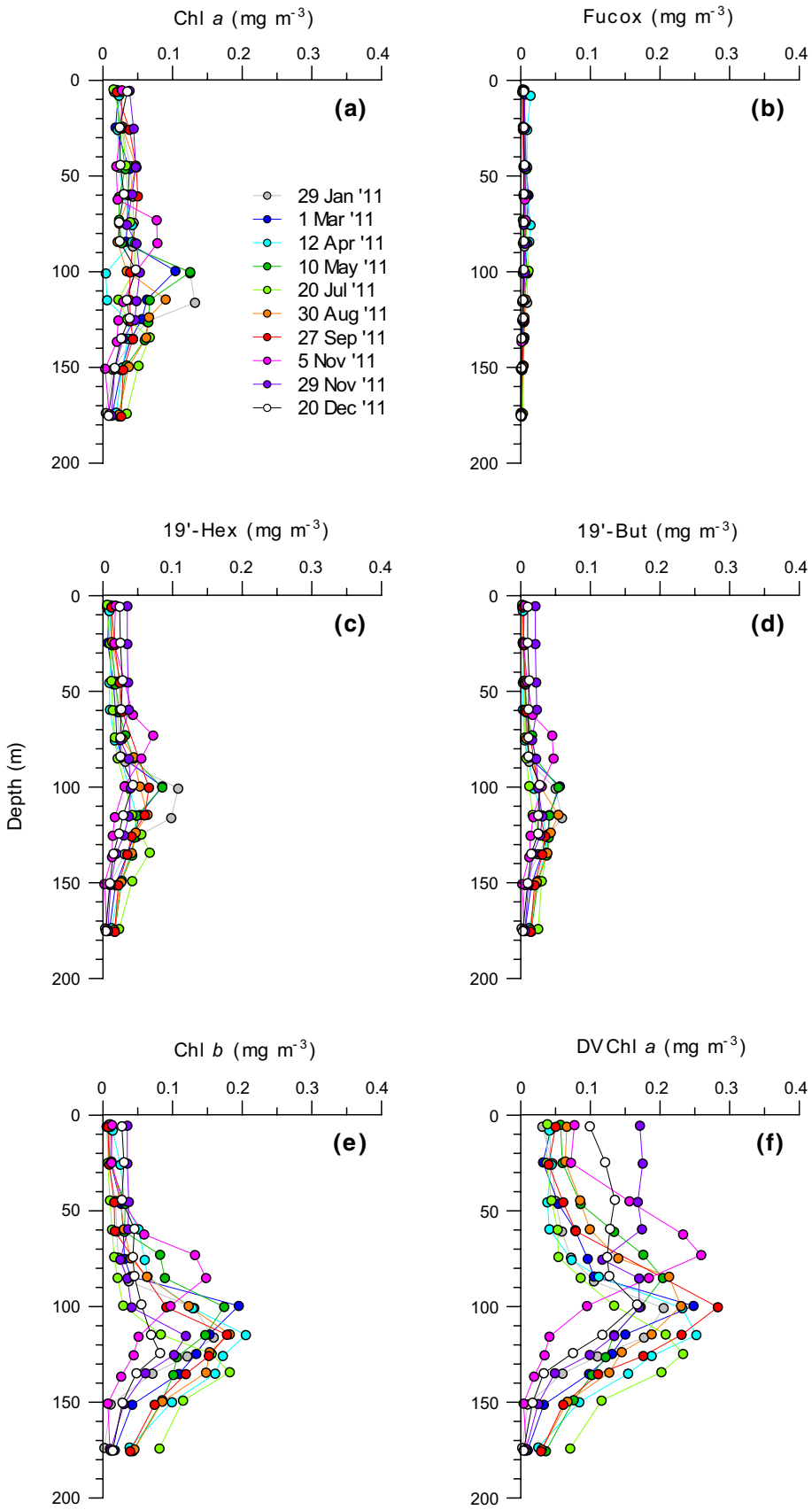

Fig. 7 Vertical profiles of concentrations of **a** Chl *a*, **b** Fucox, **c** 19′-Hex, **d** 19′-But, **e** Chl *b*, and **f** DVChl *a* at Sta. ALOHA in 2011

Shipboard observations were made six times (twice during each cruise) during the mixing period: in February 2010 and in February and April–May 2011. These observations detected distinct phytoplankton blooms in February 2011, mainly due to increases in diatoms, chlorophytes, prymnesiophytes, and chrysophytes (Table 3). However, the contribution of diatoms was relatively low (2–7 %) in the blooms that occurred in February 2010 and April–May 2011, although the remaining three groups consistently accounted for >11 % during the period. Therefore, the occurrence of spring blooms every year in this region is probably caused by an increase of chlorophytes, prymnesiophytes, and chrysophytes. On the other hand, a time series of Chl *a* maps around Sta. S1 from MODIS showed that the increase in surface Chl *a* between mid-February and mid-April was relatively high in 2004 and 2011 as compared to other years (Fig. 2c), indicating the occurrence of prominent blooms in these years. In February 2011, when our observations detected the prominent blooms, $NO_3 + NO_2$ concentrations exceeded 0.5 μmol kg^{-1} even in the surface waters due to influxes of nutrient-rich deep waters (Fig. 3e). Thus, although further detailed study is required, a greater supply of nutrients from deep waters due to sporadic physical perturbations (e.g., strong winds and mesoscale eddies) may be a likely reason for the occurrence of larger-than-normal spring blooms due to an increase of diatoms.

4 Conclusions

The NPSG has generally been considered to support a homogenous and stable phytoplankton community structure throughout the year. However, our study suggests that the abundance and composition of the phytoplankton community in the northwestern region of the NPSG are seasonally variable and are related to the overall seasonal physical forcing (i.e., deep vertical mixing and strong stratification) of the upper ocean habitat in this region. As was the case at Sta. ALOHA, *Prochlorococcus* was the greatest contributor to total Chl *a* standing stock during the stratification period at Sta. S1. An interesting observation of this study is the fact that diverse phytoplankton groups at Sta. S1 were ubiquitously present throughout the mixing and stratification periods, as compared to Sta. ALOHA. At Sta. S1, a deepening of the mixed layer in winter increased the availability of nutrients in the euphotic zone, leading to the occurrence of spring phytoplankton blooms composed of diverse groups including prymnesiophytes, chlorophytes, chrysophytes, prasinophytes, and/or diatoms. The seasonal variations of phytoplankton biomass and species composition related to the physical forcing likely affects biogeochemical processes in this region.

Acknowledgments We thank the captain and crew of the R/V *Mirai* for their support during the cruise and the staff of Marine Works Japan and Global Ocean Development for their on-board analysis and deck work. We also thank M. C. Honda and two anonymous reviewers for comments and suggestions on this manuscript. This work was carried out as part of the K2S1 project funded by the Environmental Biogeochemical Cycle Research Program of the Japan Agency for Marine-Earth Science and Technology.

References

Andersen RA, Bidigare RR, Keller MD, Latasa M (1996) A comparison of HPLC pigment signatures and electron microscopic observations for oligotrophic waters of the North Atlantic and Pacific Oceans. Deep Sea Res II 43:517–537. doi:10.1016/0967-0645(95)00095-X

Campbell L, Vaulot D (1993) Photosynthetic picoplankton community structure in the subtropical North Pacific Ocean near Hawaii (station ALOHA). Deep Sea Res I 40:2043–2060. doi:10.1016/0967-0637(93)90044-4

Cleveland JS, Perry MJ (1987) Quantum yield, relative specific absorption and fluorescence in nitrogen-limited *Chaetoceros gracilis*. Mar Biol 94:489–497. doi:10.1007/BF00431395

Corno G, Letelier RM, Abbott MR, Karl DM (2008) Temporal and vertical variability in photosynthesis in the North Pacific subtropical gyre. Limnol Oceanogr 53:1252–1265. doi:10.4319/lo.2008.53.4.1252

de Boyer Montégut C, Madec G, Fischer AS, Lazar A, Iudicone D (2004) Mixed layer depth over the global ocean: an examination of profile data and a profile-based climatology. J Geophys Res 109:C12003. doi:10.1029/2004JC002378

Eppley RW, Renger EH, Venrick EL, Mullin MM (1973) A study of plankton dynamics and nutrient cycling in the central gyre of the North Pacific Ocean. Limnol Oceanogr 18:534–551. doi:10.4319/lo.1973.18.4.0534

Fujiki T, Hosaka T, Kimoto H, Ishimaru T, Saino T (2008) In situ observation of phytoplankton productivity by an underwater profiling buoy system: use of fast repetition rate fluorometry. Mar Ecol Prog Ser 353:81–88. doi:10.3354/meps07151

Fujiki T, Matsumoto K, Saino T, Wakita M, Watanabe S (2013) Distribution and photo-physiological condition of phytoplankton in the tropical and subtropical North Pacific. J Oceanogr 69:35–43. doi:10.1007/s10872-012-0153-5

Furuya K (1990) Subsurface chlorophyll maximum in the tropical and subtropical western Pacific Ocean: vertical profiles of phytoplankton biomass and its relationship with chlorophyll *a* and particulate organic carbon. Mar Biol 107:529–539. doi:10.1007/BF01313438

Furuya K, Hayashi M, Yabushita Y (1998) HPLC determination of phytoplankton pigments using N, *N*-dimethylformamide. J Oceanogr 54:199–203. doi:10.1007/BF02751695

Geider RJ, Greene RM, Kolber Z, MacIntyre HL, Falkowski PG (1993) Fluorescence assessment of the maximum quantum efficiency of photosynthesis in the western North Atlantic. Deep Sea Res I 40:1205–1224. doi:10.1016/0967-0637(93)90134-O

Hashihama F, Kanda J, Maeda Y, Ogawa H, Furuya K (2014) Selective depressions of surface silicic acid within cyclonic mesoscale eddies in the oligotrophic western North Pacific. Deep Sea Res I 90:115–124. doi:10.1016/j.dsr.2014.05.004

Karl DM (1999) A sea of change: biogeochemical variability in the North Pacific subtropical gyre. Ecosystems 2:181–214. doi:10.1007/s100219900068

Karl DM, Lukas R (1996) The Hawaii ocean time-series (HOT) program: background, rationale and field implementation. Deep Sea Res II 43:129–156. doi:10.1016/0967-0645(96)00005-7

Karl DM, Winn CD (1991) A sea of change: monitoring the oceans' carbon cycle. Environ Sci Technol 25:1977–1981. doi:10.1021/es00024a600

Kolber ZS, Prášil O, Falkowski PG (1998) Measurements of variable chlorophyll fluorescence using fast repetition rate techniques: defining methodology and experimental protocols. Biochim Biophys Acta 1367:88–106. doi:10.1016/S0005-2728(98)00135-2

Latasa M (2007) Improving estimations of phytoplankton class abundances using CHEMTAX. Mar Ecol Prog Ser 329:13–21. doi:10.3354/meps329013

Latasa M, Scharek R, Vidal M, Vila-Reixach G, Gutiérrez-Rodríguez A, Emelianov M, Gasol JM (2010) Preferences of phytoplankton groups for waters of different trophic status in the northwestern Mediterranean Sea. Mar Ecol Prog Ser 407:27–42. doi:10.3354/meps08559

Letelier RM, Bidigare RR, Hebel DV, Ondrusek M, Winn CD, Karl DM (1993) Temporal variability of phytoplankton community structure based on pigment analysis. Limnol Oceanogr 38:1420–1437. doi:10.4319/lo.1993.38.7.1420

Li B, Karl DM, Letelier RM, Church MJ (2011) Size-dependent photosynthetic variability in the North Pacific subtropical gyre. Mar Ecol Prog Ser 440:27–40. doi:10.3354/meps09345

Mackey MD, Mackey DJ, Higgins HW, Wright SW (1996) CHEMTAX, a program for estimating class abundances from chemical markers: application to HPLC measurements of phytoplankton. Mar Ecol Prog Ser 144:265–283. doi:10.3354/meps144265

Miki M, Ramaiah N, Takeda S, Furuya K (2008) Phytoplankton dynamics associated with the monsoon in the Sulu Sea as revealed by pigment signature. J Oceanogr 64:663–673. doi:10.1007/s10872-008-0056-7

Oka E, Qiu B (2012) Progress of North Pacific mode water research in the past decade. J Oceanogr 68:5–20. doi:10.1007/s10872-011-0032-5

Ryther JH (1956) Photosynthesis in the ocean as a function of light intensity. Limnol Oceanogr 1:61–70. doi:10.4319/lo.1956.1.1.0061

Siswanto E, Matsumoto K, Honda MC, Fujiki T, Sasaoka K, Saino T (2015) Reappraisal of meridional differences of factors controlling phytoplankton biomass and initial increase preceding seasonal bloom in the northwestern Pacific Ocean. Remote Sens Environ 159:44–56. doi:10.1016/j.rse.2014.11.028

Suzuki R, Ishimaru T (1990) An improved method for the determination of phytoplankton chlorophyll using *N*, *N*-dimethylformamide. J Oceanogr Soc Jpn 46:190–194. doi:10.1007/BF02125580

Suzuki K, Handa N, Kiyosawa H, Ishizaka J (1995) Distribution of the prochlorophyte *Prochlorococcus* in the central Pacific Ocean as measured by HPLC. Limnol Oceanogr 40:983–989. doi:10.4319/lo.1995.40.5.0983

Welschmeyer NA (1994) Fluorometric analysis of chlorophyll *a* in the presence of chlorophyll *b* and pheopigments. Limnol Oceanogr 39:1985–1992. doi:10.4319/lo.1994.39.8.1985

Zapata M, Rodríguez F, Garrido JL (2000) Separation of chlorophylls and carotenoids from marine phytoplankton: a new HPLC method using a reversed phase C8 column and pyridine-containing mobile phases. Mar Ecol Prog Ser 195:29–45. doi:10.3354/meps195029